

## Description

A resonant inductive position sensor for measuring over a full 360° of rotation. Works with CambridgeIC's Central Tracking Unit (CTU) chips to provide high-quality position data to a host device.

The sensor has two sets of sensor coils: one for taking fine incremental measurements at high accuracy and resolution and another for coarse, absolute measurements. The sensor is Type 6, Subtype 3 (Type "6.3").

The sensor is connected to a CambridgeIC CTU chip, which combines the information from both sets of coils to deliver an absolute, high accuracy and high resolution output to a host system.

## Features

### Sensor

- Full absolute sensing over 360°
- 6-layer PCB process
- 15mm hole, e.g. for through shaft
- 34.2mm diameter copper coil pattern
- Target can be sensed from front or rear of PCB

### Target

- Simple design using 2 wound ferrite rods
- Balanced for immunity to misalignment
- No hole required for the rotating shaft: can be mounted from the side

## Performance

Table 1

|                            | Condition |                                   |           |
|----------------------------|-----------|-----------------------------------|-----------|
|                            | Best      | Realistic installation tolerances | Big Gap   |
| Gap Sensor to Target Coils | 0.5mm     | 1.0±0.5mm                         | 5mm       |
| Radial Misalignment        | 0mm       | 0.5mm                             | 0.5mm     |
| Angular Misalignment       | 0°        | ±0.3°                             | ±0.3°     |
| Result                     |           |                                   |           |
| Max Linearity Error        | ±0.15°    | ±0.2°                             | ±0.24°    |
| Noise Free Resolution      | 14 bits   | 13.4 bits                         | 11.5 bits |

## Applications

- Azimuth and tilt sensing for surveillance cameras
- Motion control
- Actuator position feedback
- Valve position sensing
- Absolute Optical Encoder replacement

| Product identification |                               |
|------------------------|-------------------------------|
| Part no.               | Description                   |
| 013-0024               | Assembled sensor              |
| 013-6001               | 6-way sensor connecting cable |
| 010-0057               | Sensor Blueprint              |

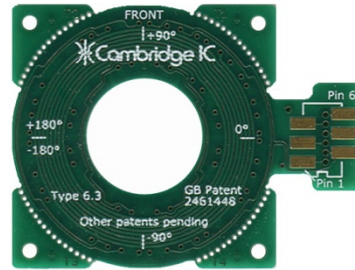


Figure 1 sensor 013-0024 (without connector)

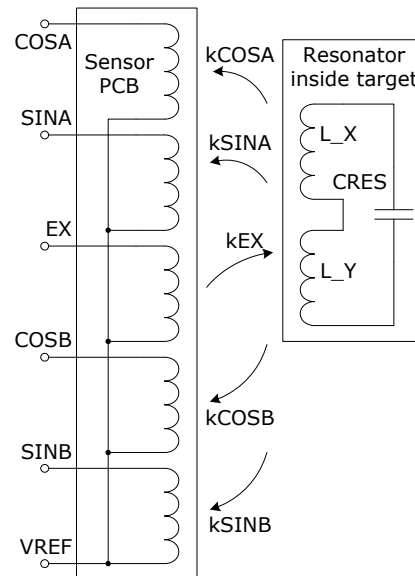


Figure 2 equivalent circuit

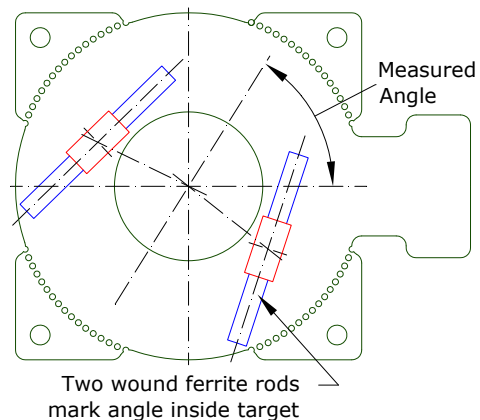
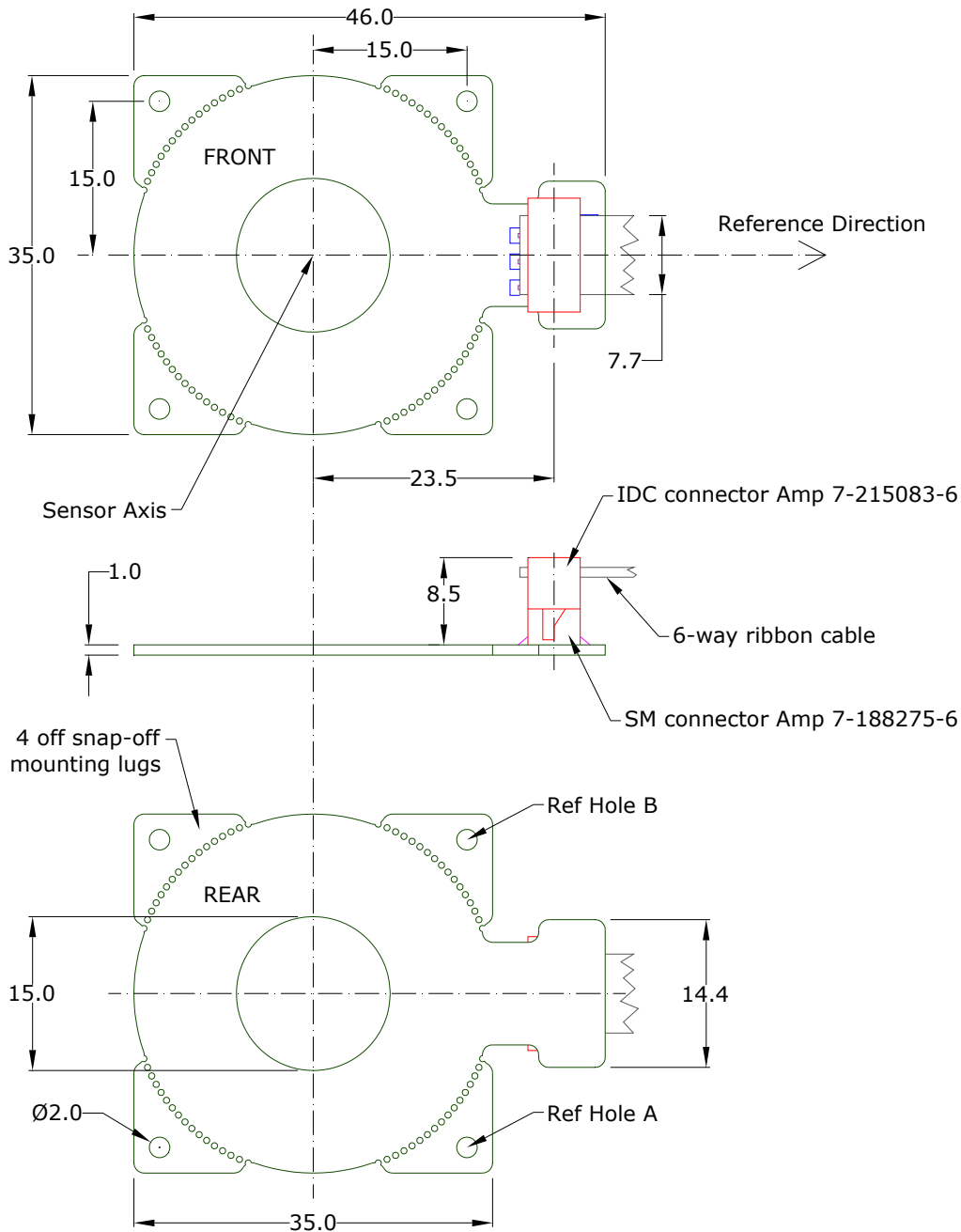


Figure 3 sensor with target components

## 1 Assembled Sensor

Figure 4 is a dimensioned drawing of the assembled sensor PCB part number 013-0024.



**Figure 4 Assembled Sensor 013-0024 shown mated with connector 013-6001**

The nominal location of the Sensor Axis is defined as 15.0mm to the left of mid way between Ref Hole A and Ref Hole B. The Reference Direction is perpendicular to the line joining the centres of these two holes.

The actual location of the Sensor Axis may be up to 0.2mm from the Nominal Sensor Axis due to hole location tolerances relative to the copper sensing pattern inherent in the PCB production process. When performance is quoted at a Radial Misalignment of 0.5mm, for example in Table 1, this 0.5mm is *in addition to* the 0.2mm misalignment between actual and Nominal Sensor Axis. In this case an allowance of 0.7mm has been made for the radial misalignment between the centroid of the copper pattern and the Target Axis.

The assembled sensor part number 013-0024 includes a connector mounted on the rear, located as shown in Figure 4. Table 2 shows signal names and their pin allocations.

**Table 2 Sensor Assembly electrical connections**

| Pin no | Signal name |
|--------|-------------|
| 1      | EX          |
| 2      | CB          |
| 3      | SB          |
| 4      | CA          |
| 5      | REF         |
| 6      | SA          |

Any of the four mounting lugs may be snapped off if required, for example to save space. Support the centre of the sensor on a flat surface with the lug overhanging an edge, grip the lug with pliers and bend the lug downwards over the edge. When all four of the lugs are removed the sensor dimensions are as shown in Figure 5.

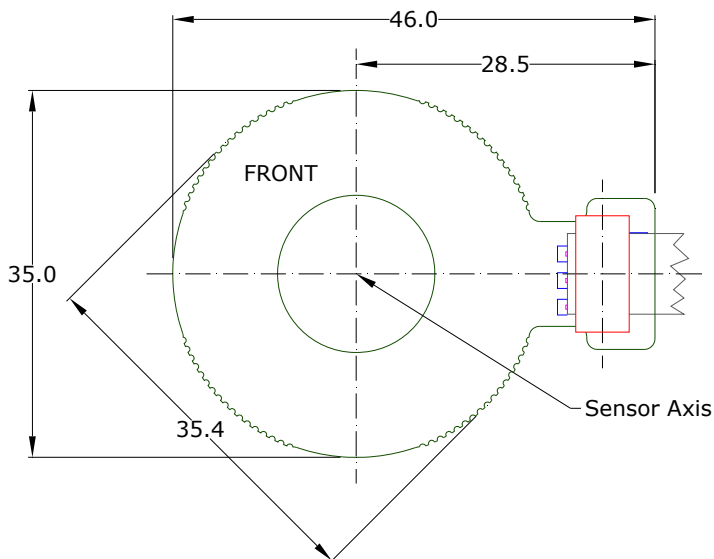


**Figure 5 Assembled sensor with mounting lugs snapped off**

## 2 Principle of Operation

The 35mm Type 6.3 Rotary Sensor measures the full, absolute angle of a target without contact, with high resolution and accuracy and with minimal influence of misalignment. This section illustrates how these features are achieved.

### 2.1 Overview

The sensor PCB comprises 5 printed coils: COSA, SINA, COSB, SINB and EX. Its equivalent circuit is illustrated in Figure 2. All 5 coils couple to a resonant circuit positioned above the sensor. The resonant circuit is the functional element inside the target, and rotates relative to the sensor.

The EX coil is for exciting this resonator. The magnetic coupling between excitation coil and resonator is uniform with rotation angle, so that the excitation coil powers the resonator whatever the rotation angle.

The other 4 coils are sensor coils, and are patterned so that their coupling factors to the resonator vary sinusoidally, as shown in section 2.3. The CTU circuit connected to the sensor detects the coupling factors and uses them to determine position.

The resonator comprises 2 wound ferrite cores placed on opposite sides of the Target Reference Direction, shown in Figure 14. This balanced arrangement is for immunity to misalignment, see section 2.4.

### 2.2 Electronic Interrogation

The sensor is connected to a CambridgeIC CTU chip (e.g. the CAM204) and its associated circuitry. To take a position measurement the CTU chip first generates a few cycles of AC current in the EX coil matching the resonant frequency of the resonator. This current forces the resonator to resonate. When the excitation current is removed the resonator continues to resonate, with its "envelope" decaying exponentially as shown in Figure 6. This decaying signal generates EMFs in the 4 sensor coils. The CTU chip detects the relative amplitude of the decaying resonator signal in each coil. It uses the amplitude information to determine position, as described below in section 2.3.

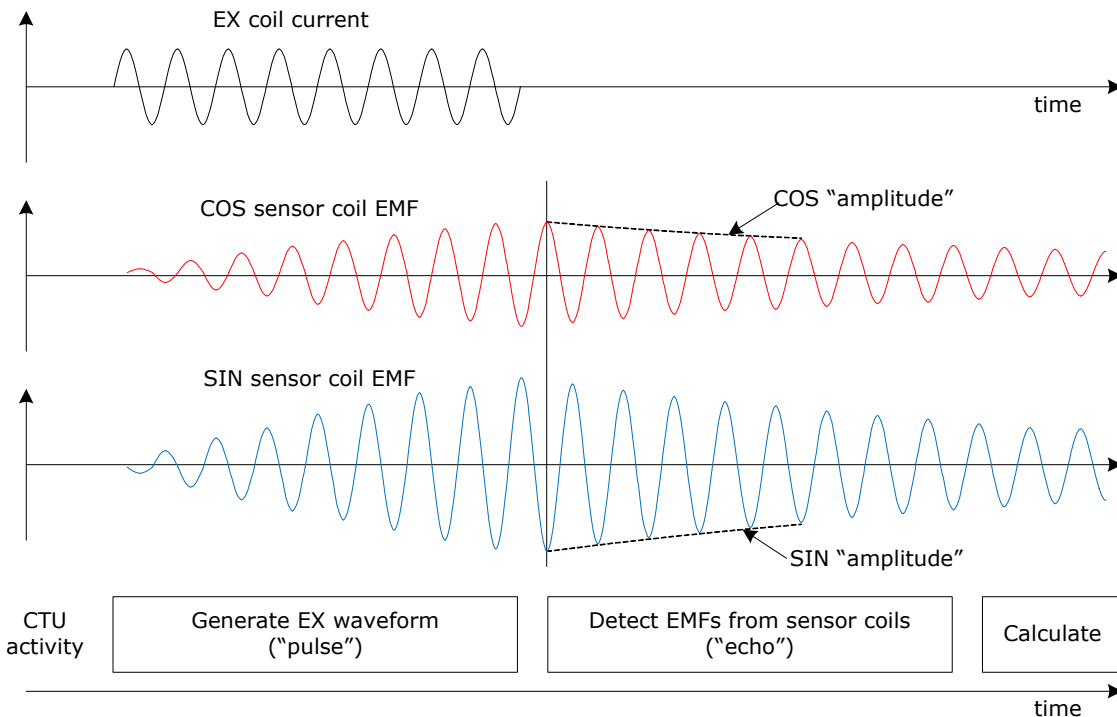


Figure 6 Electronic interrogation process

### 2.3 Sensor Coils and Position Calculation

Section 2.2 described how the CambridgeIC CTU chip detects the relative amplitude of the signals induced by the resonator in the sensor's 4 sensor coils. These measured amplitudes are proportional to the coupling factors between the resonator and each of the 4 sensor coils,  $k_{\text{COSA}}$ ,  $k_{\text{SINA}}$ ,  $k_{\text{COSB}}$ ,  $k_{\text{SINB}}$ . This subsection describes how these coupling factors change with measured angle, and the calculation the CTU chip performs to determine this angle.

Figure 7 is a simplified illustration of the sensor board's excitation coil (EX). The CTU circuit energises the target by driving a current in the EX coil. This generates a magnetic field which is positive ("+" ) inside the inner loops, and negative ("-") outside. The target's wound ferrite rods lie across the excitation coil, angled so that excitation field flows through them from the inside to the outside of the sensor. The ends of the ferrite rods are thus magnetised by the excitation field, with the inner portions of the ferrite rods having positive polarity and the outside having negative polarity. The coupling between the excitation coil and the wound ferrite rods in the target is uniform with Actual Angle, so that the target is uniformly powered irrespective of angle.

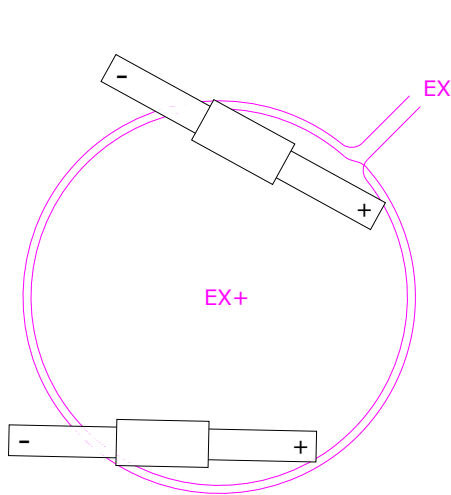


Figure 7 EX Coil, simplified

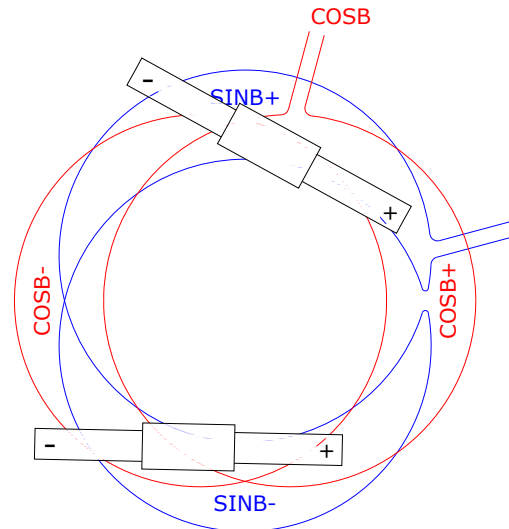


Figure 8 COSB and SINB coils, simplified

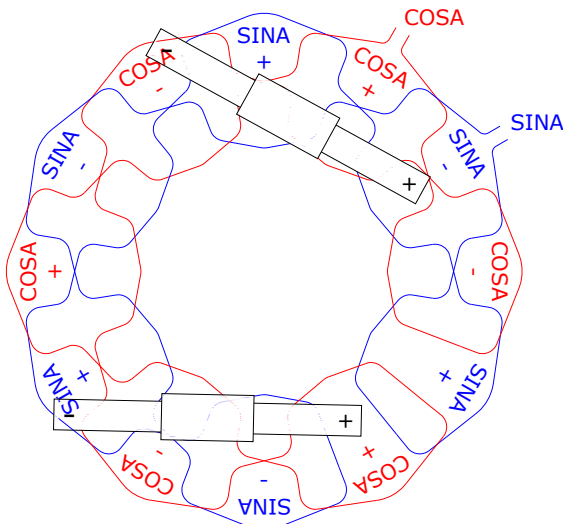


Figure 9 COSA and SINA coils, simplified

A simplified version of the COSB and SINB coils are shown in Figure 8 together with the wound ferrite rods of the target. The COSB coil is patterned to generate an output whose amplitude varies sinusoidally with Actual Angle, and having one sinusoidal repeat per circle ( $\text{SinLengthB}=360^\circ$ ). The SINB coil is similar, only mechanically rotated by  $90^\circ$  to generate an output in the SINB coil whose amplitude varies in phase quadrature with the Actual Angle.

The net coupling factors  $k\text{COSB}$  and  $k\text{SINB}$  vary in a sinusoidal fashion with Actual Angle as shown in Figure 10. The CTU chip measures  $k\text{COSB}$  and  $k\text{SINB}$  and determines *coarse position* from a 4-quadrant inverse tangent function. Coarse position is an approximate measure of angle. It is absolute across  $360^\circ$ .

The fine sensor coils,  $\text{COSA}$  and  $\text{SINA}$ , are shown simplified in Figure 9. They are superimposed on the EX,  $\text{COSB}$  and  $\text{SINB}$  coils. They are patterned for sinusoidal variation in coupling with angle, but this time with 3 sinusoidal repeats per  $360^\circ$  ( $\text{SinLengthA} = 120^\circ$ ). This number, 3 sinusoidal repeats per circle, is the sensor's Subtype.

At the Actual Angle illustrated in Figure 9, the signal amplitude measured in the  $\text{SINA}$  coil is negative, since the + ends of the wound ferrite rods are close to the  $\text{SINA-}$  lobes, and the - ends of the wound ferrite rods are close to the  $\text{SINA+}$  lobes. The signal amplitude measured in the  $\text{COSA}$  coil has a similar magnitude but is positive.

The net coupling factors  $k\text{COSA}$  and  $k\text{SINA}$  vary with Actual Angle as shown in Figure 10. The CTU chip measures  $k\text{COSA}$  and  $k\text{SINA}$  and determines *fine position* from a 4-quadrant inverse tangent function. Fine Position is a precise measure of Actual Angle, but it is incremental across  $360^\circ$ , repeating 3 times ( $\text{SinLengthA} = 120^\circ$ ). The 4-quadrant inverse tangent calculation is ratiometric so that the system is immune to changes in amplitude, for example due to changes in gap and temperature.

The CTU chip combines fine and coarse position indications, so that its final output to the host has the accuracy and resolution of the "fine" reading and full absolute information from the "coarse".

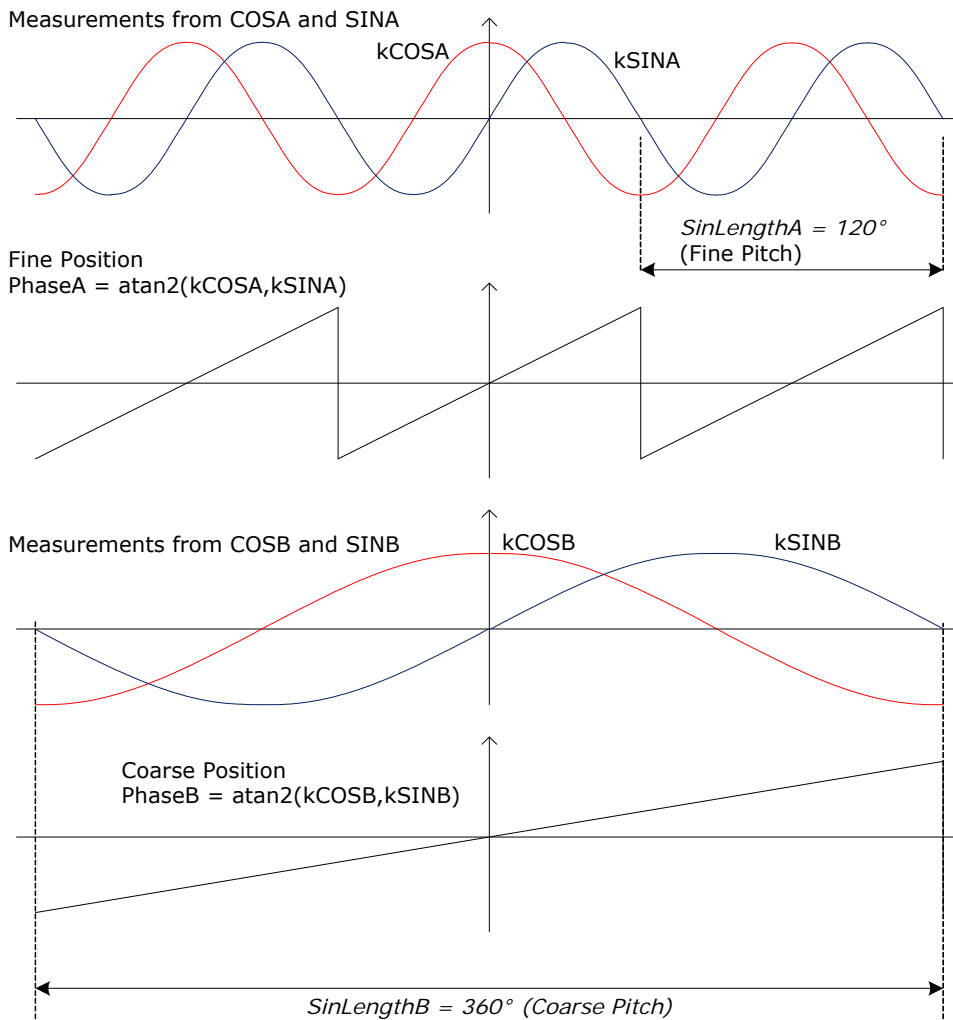


**Figure 10 sensor coil coupling factors and position calculation for Type 6.3 sensor**

## 2.4 Immunity to Misalignment

The target described in section 3 comprises two wound ferrite rods which are on opposite sides of the Sensor Axis. This makes the system largely immune to Radial Misalignment between the Target Origin and Sensor Axis.

The reason for this immunity is illustrated in Figure 11. Two target locations are shown, having the same Actual Angle but one without misalignment (wound ferrite rods shown in white) and one with Radial Misalignment (wound ferrite rods in grey). The effective angle of wound ferrite rod X shifts by an amount *Angle X Shift*, and of wound ferrite rod Y by *Angle Y Shift*. The system does not independently measure the effective angle of each wound ferrite rod; by design it measures the average of the two. And since *Angle X Shift* is approximately equal and opposite to *Angle Y Shift*, the two cancel leaving the system reporting approximately the same angle, unaffected by the Radial Misalignment.

The effect of Radial Misalignment is greater in the presence of angular misalignment between the target and Sensor Axes, in the AXr direction (AXr is defined in Figure 15). In this case wound ferrite rods X and Y are no longer the same distance to the sensor, so that their relative contributions to the system's angle measurement is no longer equal and the cancellation of *Angle X Shift* with *Angle Y Shift* is no longer so precise. This is why the sensor's performance is determined in the presence of both radial and angular misalignment to yield practical, worst-case figures (Table 1, section 5).

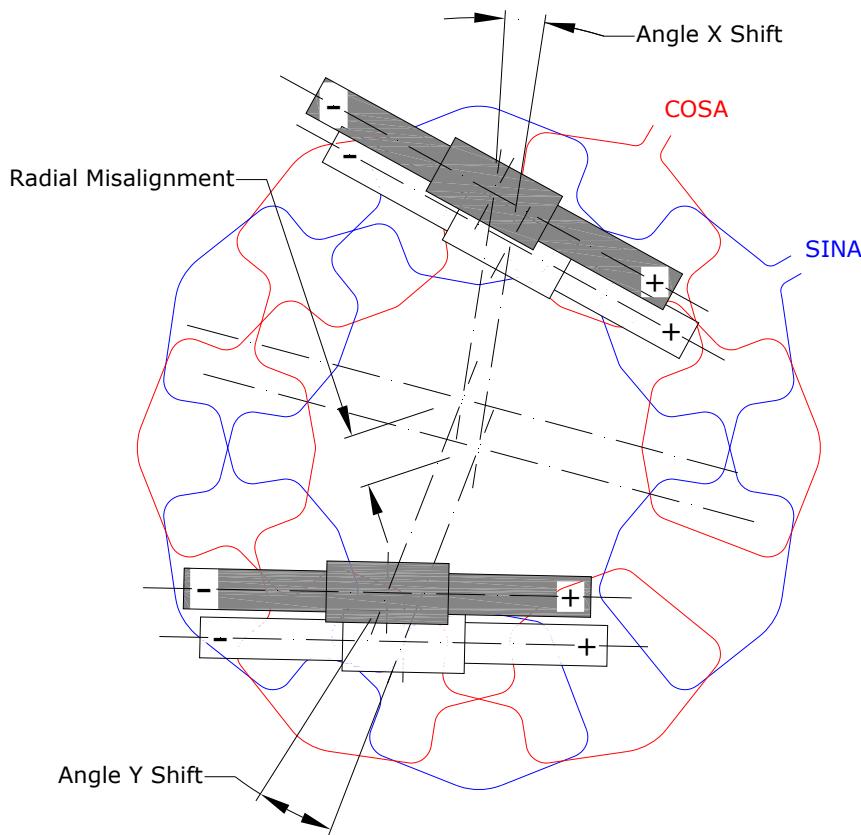


Figure 11 immunity to misalignment

Radial Misalignment causes a much larger change in coarse position, since the coarse sensor coils detect a different location on each ferrite rod which is not balanced in the same way. However this has no effect on the reported position, because the coarse coils are only used to detect position to within one fine period. Absolute position reported by the CTU chip comes only from the fine sensor coils, and there is minimal change in reported position for small lateral misalignments. However very large misalignments can cause errors in reported position readings (section 5.4), and the sensor and target should be mounted to avoid these extremes.

### 3 Target Design

This section defines the design of a target that is compatible with the 35mm Type 6.3 Rotary Sensor. The design presented here yields best immunity to misalignment, as described in section 2.4. This is done in such a way that the target can still be mounted to a rotating shaft from the side, without the shaft having to pass through a hole in the target.

#### 3.1 Wound Ferrite Rod Design

The target's functional elements are two windings around ferrite rods connected in series with a capacitor to form a resonant circuit. The two wound ferrite rods X and Y, are built to an identical specification (Table 3), with the mechanical outline illustrated in Figure 12.

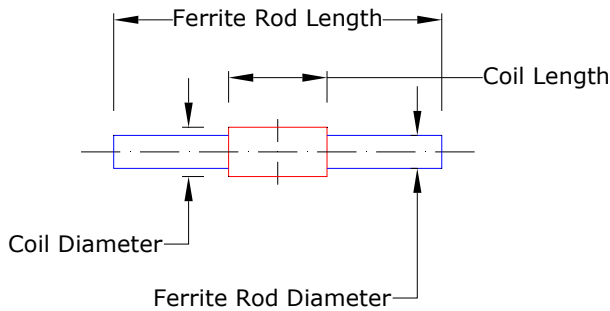


Figure 12 Design of Wound Ferrite Rods X and Y

#### 3.2 Electrical Design

Two windings are connected together with a resonating capacitor as shown in Figure 13. There are two possible connection schemes: series or parallel. In each case the nominal inductances of the two wound ferrites should be the same:  $L_S$  for series connection and  $L_P$  for parallel. The effective inductance of the connected windings  $L_{RES}$  equals twice  $L_S$  or half  $L_P$ .

The coil winding directions must be the same, so that current flowing in both coils generates field in the directions marked in Figure 14. The combination forms a resonant circuit with resonant frequency  $F_{res}$  given by:

$$F_{res} = \frac{1}{2\pi\sqrt{C_{RES} \times L_{RES}}}$$

Equation 1

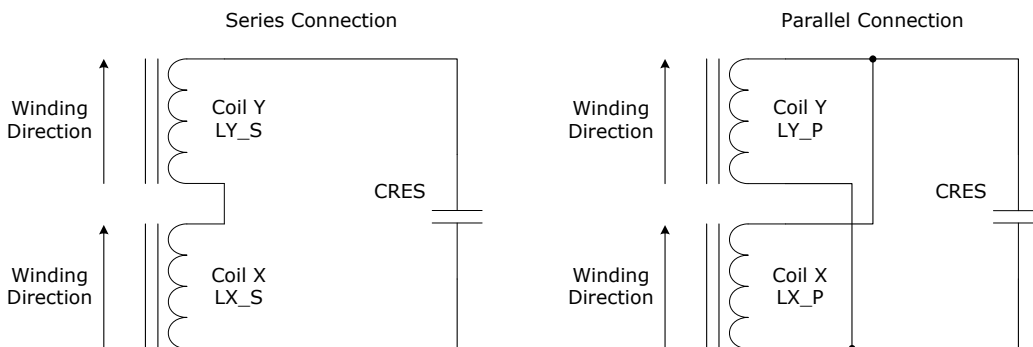
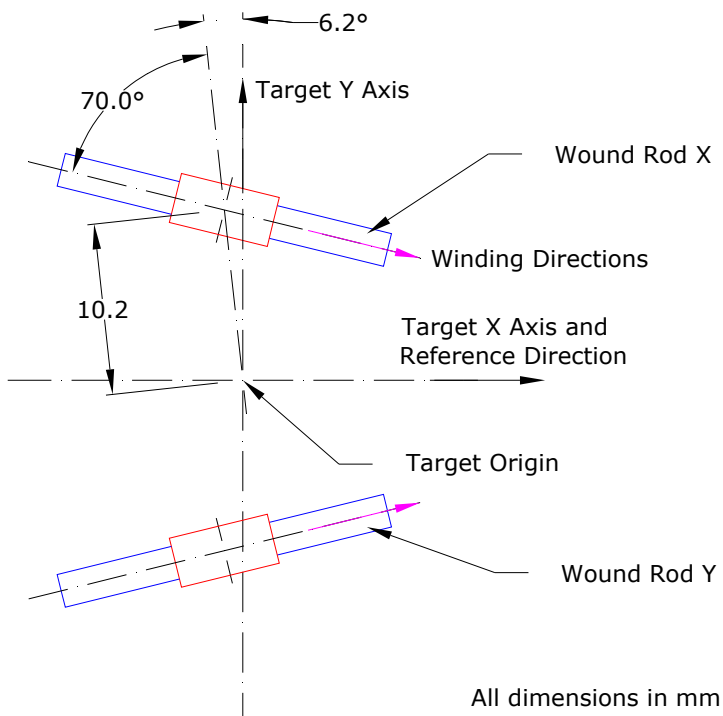


Figure 13 Electrical Schematic

### 3.3 Wound Ferrite Rod Locations on Target

The two wound ferrite rods should be attached to a suitable housing which maintains their relative locations illustrated in Figure 14. This arrangement is for immunity to misalignment between the sensor and target, see section 2.4.



**Figure 14 Location of Wound Ferrite Rods X and Y**

In use, the sensor measures the angle of the Target Reference Direction relative to the Sensor Reference Direction shown in Figure 4.

### 3.4 Specifications

Table 3 lists the primary specifications for the target, which must be met for correct function and performance. The exact dimensions of the coils, the wire diameter and the number of turns can all be varied to suit available winding wire and capacitor values.

**Table 3 Primary specifications for target**

| Parameter                        | Value         | Comments  |
|----------------------------------|---------------|---|
| Ferrite Rod Length               | 20.0±0.9mm    |   |
| Ferrite Rod Diameter             | 2.0±0.1mm     |   |
| Ferrite Rod permeability $\mu_r$ | 1000 min      | Bulk material permeability  |
| Coil Length                      | 7.0±1.0mm     |   |
| Max Coil Offset                  | ±0.5mm        | Centre of coil to centre of ferrite rod   |
| Resonator Q-factor               | >100          | Across required temperature range.  |
| Resonator Frequency $F_{res}$    | 187.5kHz ± 4% | To meet ±7% CTU tuning range and allowing ±3% frequency change in use. Measured in metal environment of product e.g. with aluminium behind. |

To achieve high Q-factor the coil diameter should be maximised within the space available, and the winding wire diameter should be kept below 0.2mm. The system's Amplitude and hence resolution is improved with higher Q-factor.

Table 4 lists actual values used for testing. These are provided as an example, but there is scope to vary the parameters within the limits defined by Table 3, for example to achieve a different capacitor value.

**Table 4 Implementation Example**

| Parameter                  | Value              | Comments   |
|----------------------------|--------------------|--|
| Ferrite Rod material       | 3B1                | Ferroxcube ROD2/20-3B1-D   |
| Ferrite Rod Length         | 20.0±0.2mm         |  |
| Ferrite Rod Diameter       | 2.00±0.05mm        |  |
| Coil Length                | 7.4mm              |  |
| Coil Diameter              | 2.8mm              |  |
| Winding wire               | 0.10mm copper dia. | Enameled self bonding  |
| Coil layers                | 4                  |  |
| Coil turns                 | 244                | Each of LX and LY  |
| Coil AC Resistance         | 7.1 $\Omega$       | LX or LY, measured at 100kHz   |
| Connection type            | Parallel           |  |
| Coil inductance            | 1030 $\mu$ H ± 3%  | LX_P or LY_P, measured at 100kHz   |
| Capacitor CRES value       | 1.5nF ± 5%         | Tolerance can be traded with inductance tolerance to deliver required frequency tolerance. |
| Capacitor material         | NPO/COG            | For high Q-factor  |
| Capacitor voltage rating   | 630V               | Peak instantaneous voltage 80V plus large safety margin                                    |
| Recommended capacitor      | FK26COG2J152J      | From TDK   |
| Q-factor, free space       | 150                | Measured at 20°C   |
| $F_{res}$ , free space     | 182kHz             |  |
| $F_{res}$ , aluminium near | 193kHz             | Placed on aluminium sheet 2.5mm from coil  |

## 4 Definitions

### 4.1 Coordinate System

The system measures the angle of a target relative to a sensor. The Target Reference Direction is the symmetry axis of the target (Figure 14). For assembled sensors, the Sensor Reference Direction is defined relative to REF Hole A and Ref Hole B shown in Figure 4. The Actual Angle is the angle between the two. Strictly, since the target may be slightly tilted relative to the sensor, Actual Angle is the angle between the projection of the Target Reference Direction onto the sensor's XY plane and the Sensor Reference Angle. This is denoted Actual Angle below.

The sensor's X Axis coincides with the Sensor Reference Direction, and its Y-Axis is orthogonal and in the plane of the sensor, as shown in Figure 15. The Z-Axis is orthogonal to X and Y Axes.

The target's X-Axis is denoted  $X_r$  and coincides with the Target Reference Direction. The target's Y-Axis,  $Y_r$ , is orthogonal to  $X_r$  and also in the plane of the ferrite rod axes. Tilt of the target relative to the sensor is defined about  $X_r$  and  $Y_r$ . It is convenient to define tilt about the target axes, since the effect of angular misalignment in the  $AY_r$  direction is significantly smaller than in the  $AX_r$  direction. References to Angular Misalignment below are therefore in the  $AX_r$  direction, so that the worst case is presented.

Radial Misalignment is the distance between the Target Origin and Nominal Sensor Axis.

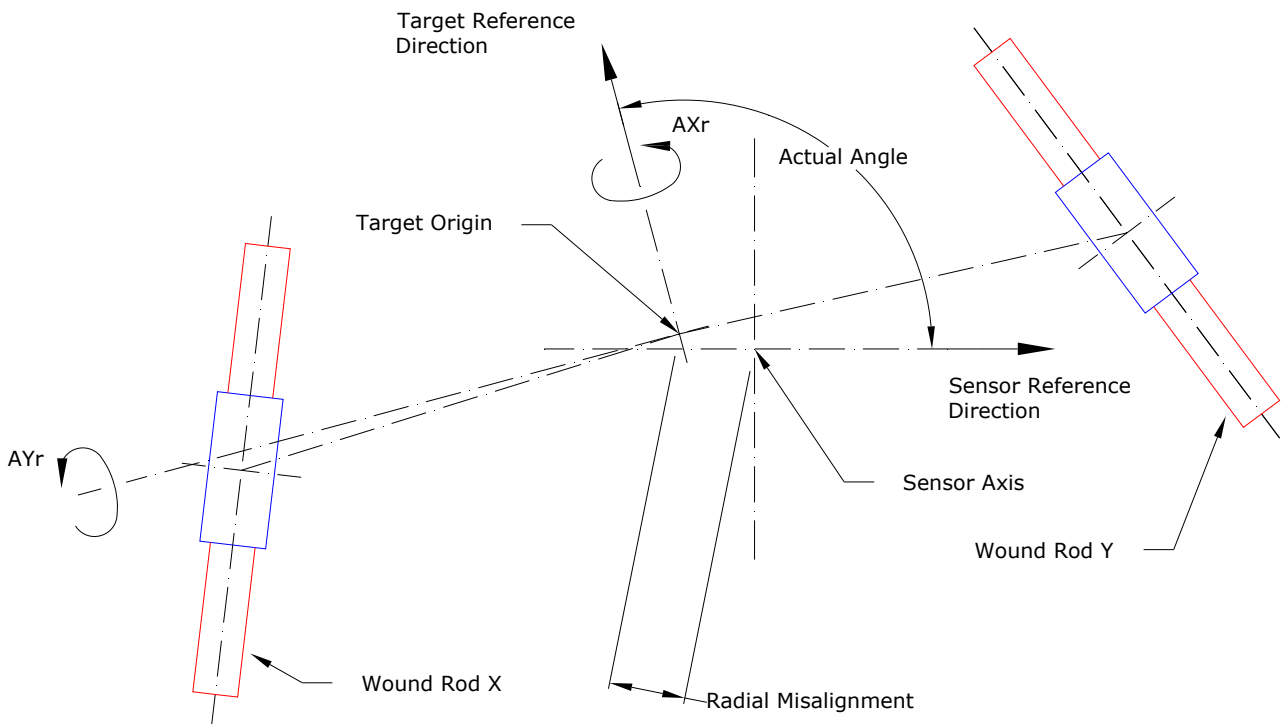


**Figure 15 Coordinate System**

Figure 16 shows how Gap is defined. It is measured 2.1mm from the centres of the ferrite rods, which makes an allowance for the radius of the coil plus housing thickness. If the target is housed in a different target then gap figures should be adjusted accordingly.

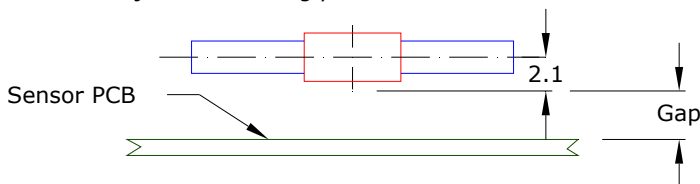


**Figure 16 Definition of Gap**

## 4.2 Transfer Function and Performance Metrics

The sensor is connected to a CTU chip which reports position as a 32-bit signed integer, here denoted *CtuReportedPositionI32*. The sensor's *Sin Length* parameter is 120°. The reported position may be converted to degrees using:

$$\text{Reported Angle in Degrees} = \frac{\text{CtuReportedPositionI32}}{65536} \times 120^\circ$$

### Equation 2

This figure is nominally equal to the Actual Angle defined in section 4.1. The figures differ due to random noise, Linearity Error and Offset Error:

$$\text{Reported Angle} - \text{Actual Angle} = \text{Random Noise} + \text{Linearity Error} + \text{Offset Error}$$

### Equation 3

## 4.3 Random Noise and Resolution

Random noise is inherent in any analog measurement. The random noise present in the CTU's reported measurements can be considered Gaussian (*well behaved noise*). There are two general measures of Random Noise, Peak to Peak Noise and Standard Deviation. Defining Peak to Peak Noise such that it encompasses 99.9% of samples (100% is physically impossible due to the statistical nature of noise) yields the following relationship:

$$\text{Peak to Peak Noise} = 6.6 \times \text{Standard Deviation}$$

### Equation 4

Another common measure of noise used in encoders is Noise Free Resolution, which is related to Peak to Peak Noise as follows:

$$\text{Noise Free Resolution} = \log_2 \frac{360^\circ}{\text{Peak to Peak Noise in }^\circ}$$

### Equation 5

Noise Free Resolution can be improved by averaging raw samples from a CTU, or applying some other digital filter to the samples. Averaging  $2^N$  samples increases Noise Free Resolution by N/2 bits. So averaging 4 samples (N=2) improves Noise Free Resolution by 1 bit, and averaging 16 (N=4) samples improves Noise Free Resolution by 2 bits. Measurements of Linearity Error and Offset Error are separated from Random Noise by averaging in this way.

## 4.4 Linearity Error and Offset Error

Linearity Error is the deviation of the transfer function from a straight line. In this case the slope of the straight line is fixed at 360° per 360° because of the continuous rotary nature of the sensor. So Linearity Error simply measures deviations relative to an Offset Error.

There are two main contributions to Offset Error: one from the sensor and one from the target.

The target's contribution to Offset Error is mainly due to the location and symmetry of its wound ferrite rods relative to the Target Reference Direction.

The sensor's contribution to Offset Error is mainly due to the PCB manufacturing process, in particular angular misregistration of layers 2, 3, 4 and 5 relative to the holes defining the Sensor Reference Angle.

## 5 Performance

Figures below are representative of assembled sensors available from CambridgeIC (as described in section 1) and of sensors built to the same specification. Measurements are taken with a typical target (built according to section 3, Table 4) and CAM204 CTU Circuitry (see CTU datasheet, grade A components), at room temperature and in free space unless otherwise stated. Sensors are mounted flush against a flat surface for test purposes.

Measurements are presented as a function of Gap, which is defined Figure 16.

### 5.1 Linearity Error

Linearity Error is defined in section 4.4. It is minimised when there is no Radial or Angular Misalignment. Figure 17 shows how Linearity Error changes with Gap and when misalignments are introduced. The quoted misalignment is *in addition* to  $\pm 0.2\text{mm}$  of misalignment between copper and REF Holes.

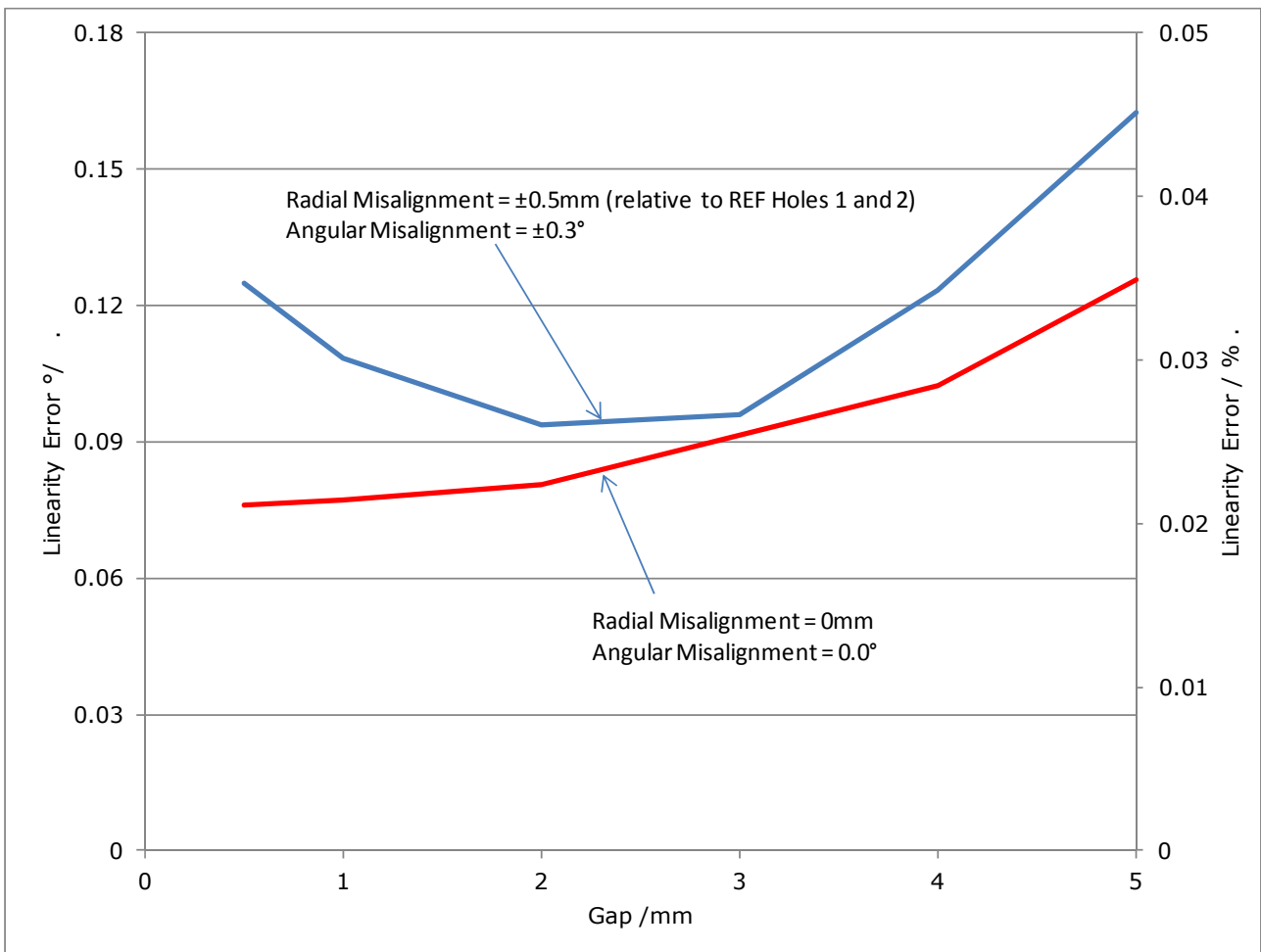


Figure 17 Linearity Error as a function of Gap and misalignment

### 5.2 Amplitude

In addition to reporting position, the CTU chip also reports Amplitude. Amplitude is a useful measure of system health, and reduces with gap as shown in Figure 18. Amplitude also reduces with the presence of nearby metal, and sensor installations should be checked to ensure any reduction is not excessive. The minimum reliably detectable Amplitude is 700.

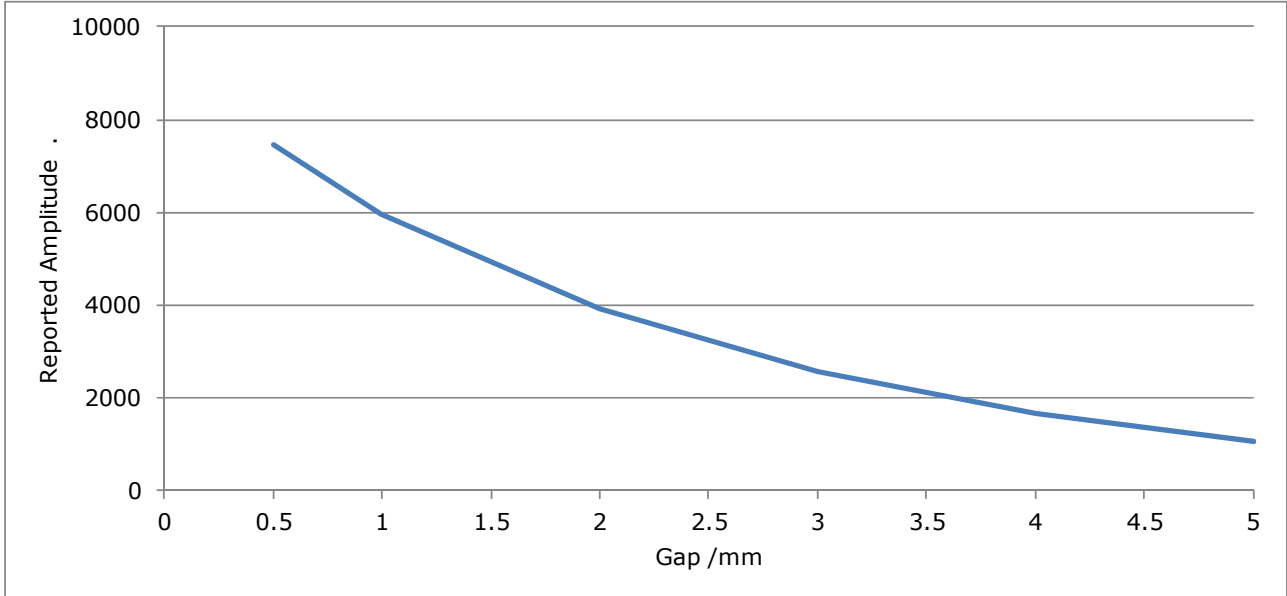


Figure 18 Minimum Reported Amplitude as a function of Gap, free space

### 5.3 Noise Free Resolution

Noise Free Resolution is defined in section 4.3. It is a function of the signal level detected by the CTU chip. It therefore reduces with gap in a similar way to Reported Amplitude as illustrated in Figure 19.

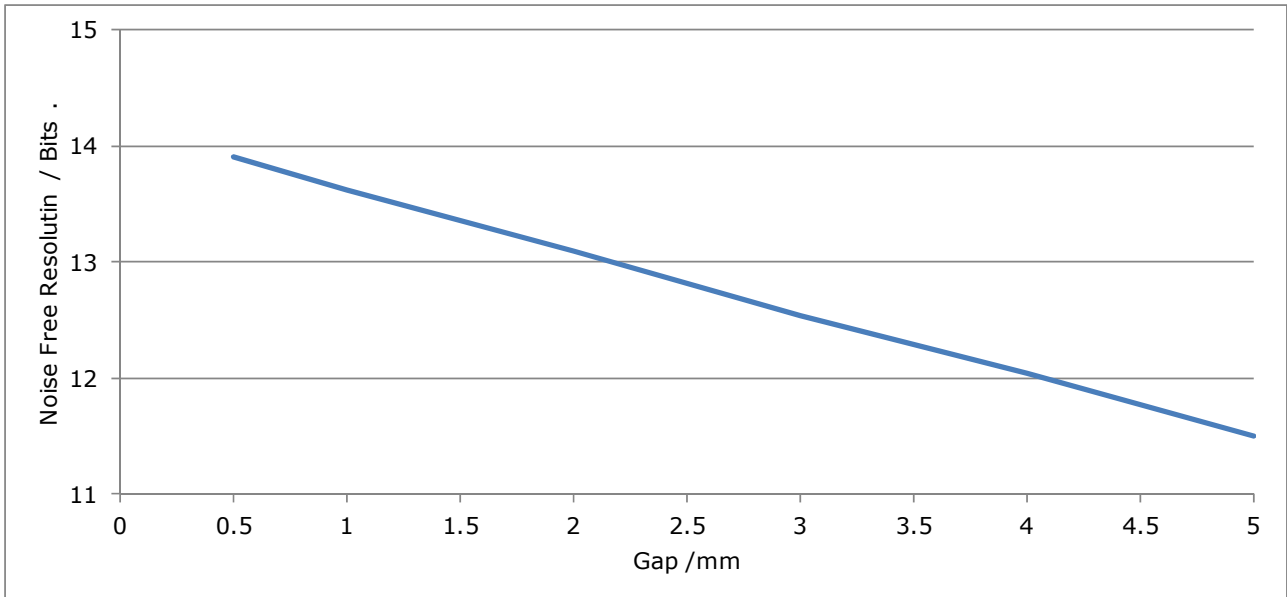


Figure 19 Noise Free Resolution as a function of Gap, CAM204 CTU chip, free space

Quoted Noise Free Resolution is based on single measurements from a CTU chip. The host may average (or otherwise digitally filter) measurements to yield a higher resolution than shown above, at the expense of greater latency.

## 5.4 Maximum Misalignment

When used with the target design detailed in section 3, the sensor will report angle correctly even when the target and sensor are badly misaligned. Table 5 shows the maximum allowable misalignments, and the resulting maximum linearity error. If radial or angular misalignment exceeds these values, for example when held by hand during demonstration, reported position may include an error of  $\pm 120^\circ$  if valid.

**Table 5 Maximum misalignment between target and sensor**

| Parameter                         | Maximum |
|-----------------------------------|---------|
| Radial Misalignment               | 2mm     |
| Angular Misalignment              | 2°      |
| Linearity Error at max alignments | 1.3°    |

## 6 Metal Integration

### 6.1 Background

As will all resonant inductive sensors, the 35mm Type 6.3 sensor and its target can be integrated near metal providing the metal's influence is not excessive.

The metal must not dampen the resonator's Q-factor excessively, and distort fields such that coupling factor is reduced excessively, otherwise Amplitude will be significantly reduced. Low Amplitude causes low Noise Free Resolution.

The resonator's resonant frequency  $F_{res}$  must also remain within the tuning limits of the CTU it will be use with (typically  $\pm 7\%$ ), and nearby metal may cause a frequency shift.

Finally, nearby metal can cause additional linearity error, although the effect is usually small, especially when the metal is placed symmetrically around the sensor.

Small metal objects such as fixing screws have less effect than larger objects and metal surfaces.

The sensor and its target are much more tolerant of nearby Aluminium and brass than steel, stainless steel or iron. If steel or iron is to be placed near the sensor and/or target and is found to cause significant Amplitude or frequency issues, then an aluminium screen is recommended between sensor and/or target and the steel at least 0.2mm thick. For example, a steel shaft can be used through the centre of the target providing it is sleeved by a thin aluminium tube.

The effect of a product's fixed metal environment is highly reproducible and can be established by experiment, for example using CambridgeIC's CTU Demo application and appropriate sensor, target and CTU Development Board.

If the product's metal environment is found to alter the target's free space resonant frequency, this may be adjusted to ensure that it is in specification when integrated with the product.

Where aluminium is required close to the rear of the sensor and is found to have a significant effect, say closer than 3mm, ferrite loaded polymer shielding material may be used, as illustrated in the following example.

### 6.2 Example: Close Integration with Aluminium

In the example illustrated in Figure 20, the sensor assembly and target are effectively surrounded by a cylinder of aluminium on all sides, except for a slot for the sensor's connections to pass through. There is also a rotating 10mm diameter aluminium shaft through the middle.

Ferrite loaded rubber polymer shield material is used to screen the sensor from the aluminium immediately behind. This material also causes a reduction in target resonant frequency, which counteracts the increase caused by the aluminium on the other sides. The material is Flexield from TDK, IRJ18AB material, 0.5mm thick.

Table 6 shows the resulting performance, measured as a function of Gap.

**Table 6 Aluminium integration example: performance**

| Parameter                               | Gap       |         |           |
|---|-----------|---------|-----------|
|   | 0mm       | 1mm     | 2mm       |
| Frequency change relative to Free Space | 0%        | +0.7%   | +1.6%     |
| Amplitude                               | 7680      | 4580    | 3340      |
| Noise Free Resolution                   | 13.5 bits | 13 bits | 12.5 bits |

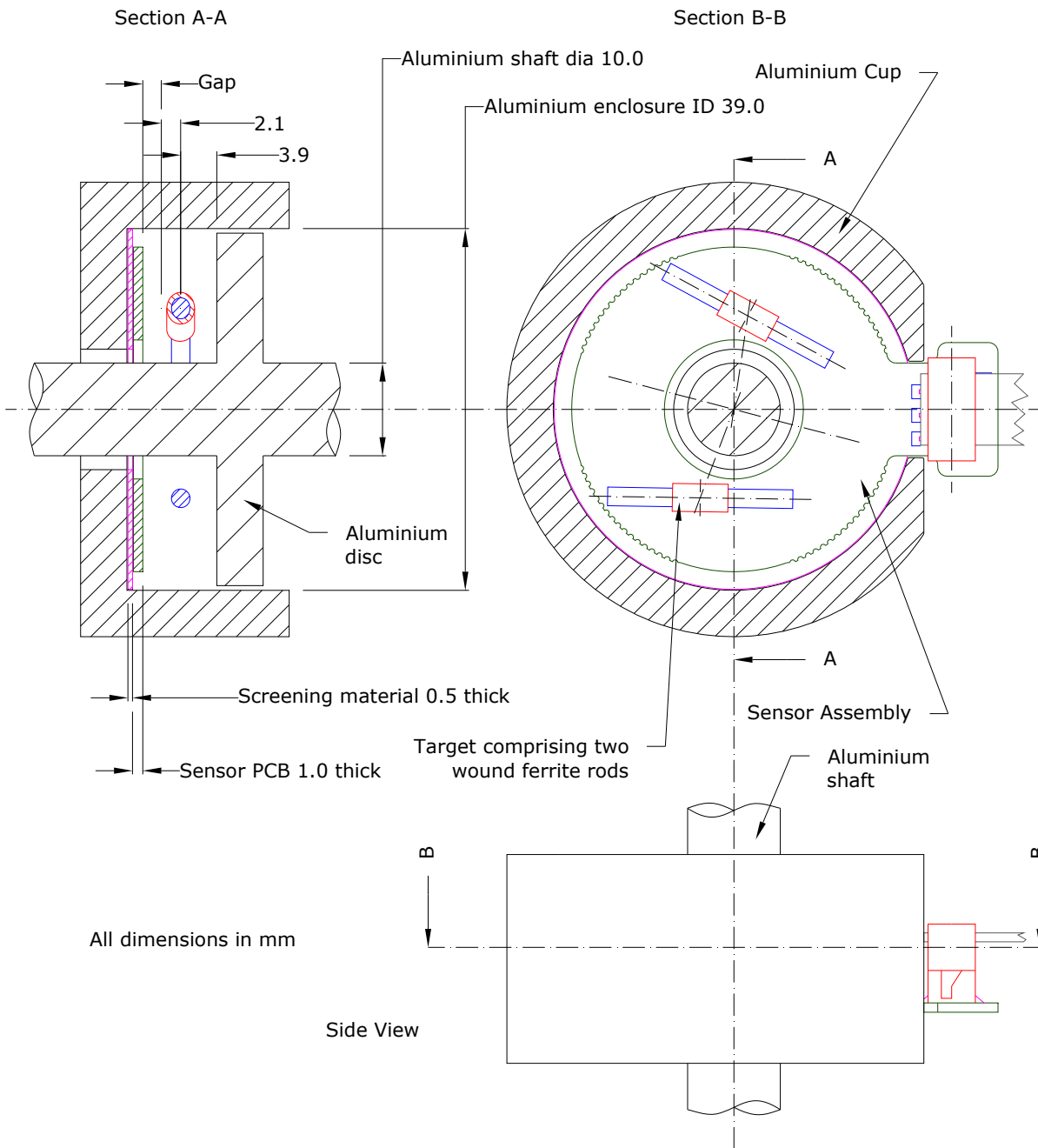


Figure 20 Metal integration example: surrounded by aluminium

## 7 Sensor Blueprint 010-0057

### 7.1 Purpose

A Sensor Blueprint is data defining the pattern of conductors for building the sensor onto a PCB. A customer may build their own sensors for use with CambridgeIC’s CTU chips, either as stand-alone sensors or combined with their own circuitry.

### 7.2 Fabrication Technology

The Sensor Blueprint is fabricated on a 6-layer PCB. Recommended copper thickness is shown in Table 7.

Table 7

| Copper thickness | oz  | µm |
|------------------|-----|----|
| Minimum          | 0.8 | 28 |
| Recommended      | 1   | 35 |

### 7.3 PCB Design Parameters

Table 8

| PCB Design Rules        | Minimum values used |        |
|-------------------------|---------------------|--------|
|                         | mm                  | inches |
| Track width             | 0.2                 | 0.0079 |
| Gap between tracks      | 0.2                 | 0.0079 |
| Via land outer diameter | 0.8                 | 0.031  |
| Drill hole diameter     | 0.4                 | 0.016  |

### 7.4 PCB Integration

Figure 21 illustrates the extent of the copper pattern required to build the sensor on a PCB. The shaded area is the sensor itself, with coil connections shown to the upper right. The coil pattern may be rotated or flipped to fit a customer’s assembly, in which case the position reported by the CTU will be transformed accordingly.

When integrating with other electronic circuitry, a keep-out of 3mm is recommended all round the sensor’s conductors.

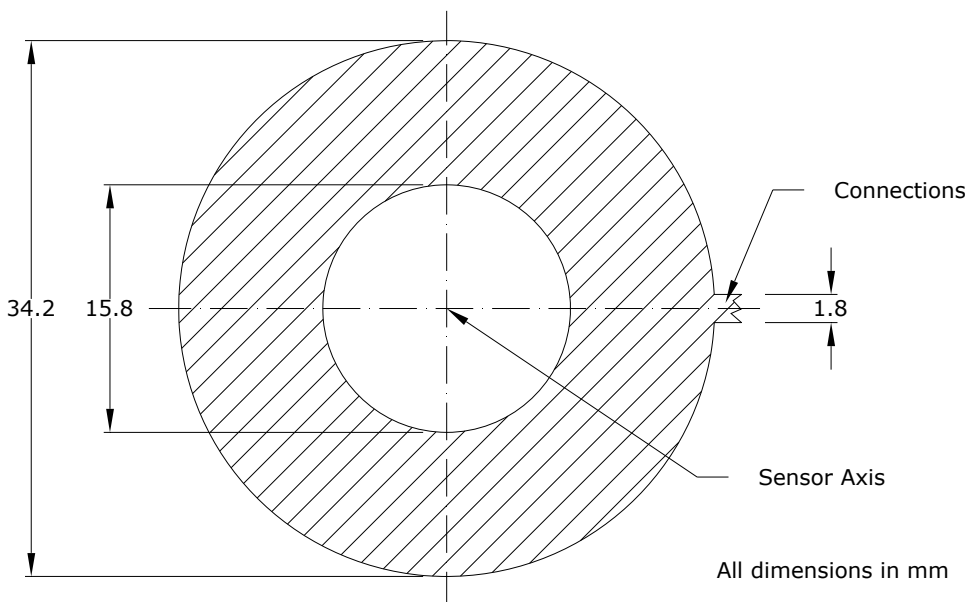


Figure 21 Copper extent

## 7.5 Data Format

The Sensor Blueprint is supplied as Gerber data in RS-274-X format with the following settings: imperial, 2.4 precision and leading zero suppression. Coordinates are relative to the Sensor Axis.

## 7.6 Trace Connections

There are 5 pairs of tracks (EX, COSA, SINA, COSB, SINB and their respective VREF connections), which should be connected to the respective CTU circuit connections with the minimum practical trace lengths.

Please refer to the CAM204 datasheet for recommendations on track design for connecting sensors to CTU circuitry.

## 8 Environmental

Assembled sensor part number 013-0023 conforms to the following environmental specifications:

| Item                          | Value | Comments                                 |
|-------------------------------|-------|--|
| Minimum operating temperature | -40°C | Limited by the wire used for connections |
| Maximum operating temperature | 85°C  |  |
| Maximum operating humidity    | 95%   | Non-condensing                           |

The maximum operating temperature may be increased if a customer manufactures their own sensor PCB to CambridgeIC's design, and uses an alternative, higher temperature, connecting method.

## 9 Document History

| Revision | Date             | Comments   |
|----------|------------------|--|
| 0001     | 10 August 2012   | First release                                    |
| 0002     | 13 August 2012   | Corrected part number of recommended capacitor   |
| 0003     | 7 September 2012 | Corrected CRES value in Table 4 (1.5nF not 1.5F) |

## 10 Contact Information

Cambridge Integrated Circuits Ltd  
 21 Sedley Taylor Road  
 Cambridge  
 CB2 8PW  
 UK

Tel: +44 (0) 1223 413500

[info@cambridgeic.com](mailto:info@cambridgeic.com)

## 11 Legal

This document is © 2012 Cambridge Integrated Circuits Ltd (CambridgeIC). It may not be reproduced, in whole or part, either in written or electronic form, without the consent of CambridgeIC. This document is subject to change without notice. It, and the products described in it ("Products"), are supplied on an as-is basis, and no warranty as to their suitability for any particular purpose is either made or implied. CambridgeIC will not accept any claim for damages as a result of the failure of the Products. The Products are not intended for use in medical applications, or other applications where their failure might reasonably be expected to result in personal injury. The publication of this document does not imply any license to use patents or other intellectual property rights. The design of the sensor, comprising each of the patterned copper layers, drill locations, silk screens, assembly layers and board outline, and of the associated target, are protected by copyright and patents. Patents include GB2461448. Other patents are pending.